

Article

Degradation of UV Filter Ethyl 4-Aminobenzoate (Et-PABA) Using a UV-Activated Persulfate Oxidation Process

Ruirui Han ¹, Qiang Wu ², Chihao Lin ², Lingfeng Zhang ², Zhicai Zhai ², Ping Sun ^{2,*} , Yingsen Fang ^{2,*}, Jiaqiang Wu ¹ and Hui Liu ^{2,*}

¹ Nanhu College, Jiaxing University, Jiaxing 314001, China

² College of Biological, Chemical Sciences and Engineering, Jiaxing University, Jiaxing 314001, China

* Correspondence: sunping@zjxu.edu.cn (P.S.); fangyingsen@zjxu.edu.cn (Y.F.); liuhui@zjxu.edu.cn (H.L.); Tel.: +86-0573-8364-6045 (P.S.); +86-0573-8364-3695 (Y.F. & H.L.)

Received: 24 June 2019; Accepted: 16 July 2019; Published: 18 July 2019



Featured Application: This work provides basic data, application references and theoretical guidance of the UV/PDS process for the removal of PABA-type UV filters in water.

Abstract: In this paper, the ultraviolet/persulfate (UV/PDS) combined oxidation process was used to remove the ethyl 4-aminobenzoate (Et-PABA), one of the typical 4-aminobenzoic acid (PABA)-type UV filters. The effects of various factors on the removal of Et-PABA using the UV/PDS process were investigated, and the degradation mechanisms of Et-PABA were explored. The results showed that the UV/PDS process can effectively remove 98.7% of Et-PABA within 30 min under the conditions: UV intensity of $0.92 \text{ mW}\cdot\text{cm}^{-2}$, an initial concentration of Et-PABA of 0.05 mM , and a PDS concentration of 2 mM . The removal rate of Et-PABA increased with the increase in PDS dosage within the experimental range, whereas humic acid (HA) had an inhibitory effect on Et-PABA removal. Six intermediates were identified based on HPLC–MS and degradation pathways were then proposed. It can be foreseen that the UV/PDS oxidation process has broad application prospects in water treatment.

Keywords: advanced oxidation processes (AOPs); UV-activated; persulfate; ethyl 4-aminobenzoate (Et-PABA)

1. Introduction

In recent years, skin cancer has attracted widespread attention owing to a series of risks related to ultraviolet (UV) radiation, sunburn, and premature skin aging [1]. Thereby UV filters are widely used in personal care products (PCPs) as UV-absorbing (shielding) agents that protect against UVA and UVB radiation and protect human health [2]. Most PCPs such as cosmetics, sunscreens, hair care products, detergents, etc., contain one or more UV filters in everyday products that are closely related to our lives. These organic UV filters are prone to the persistent pollution of the environment due to their large dosage, stable physical and chemical properties, and resistance to degradation. Those UV filters have become a new class of contaminants as they continue to enter the environment daily [3]. Residues of organic UV filters have been detected in various media such as surface water, sediment and aquatic organisms [4–7]. Several studies have shown that UV filters have potential endocrine disrupting effects that adversely affect organisms such as human tissues, mammals, animals, and fish, and cause serious health threats [8–11]. UV filters are relatively stable in nature and are resistant to biodegradation, making it difficult for municipal wastewater treatment plants (MWTPs) to remove them thoroughly [12–14]. Among them, *p*-aminobenzoic acid (PABA)-type compounds are the earliest and most widely used sunscreen products, thus their exposure characteristics, ecological effects and

environmental behavior have become research hotspots in environmental fields in recent years [15,16]. They can exist for a long time and are dispersed in the environment due to their relatively high photochemical stability and low biodegradability. Thus, it is urgent to find efficient ways to remove PABA-type UV filters thoroughly.

In recent years, advanced oxidation technology based on sulfate radicals (SR-AOPs) has become a new research hotspot, and it has some practical applications at home and abroad [17]. Persulfate (PS), used to produce sulfate radicals ($\text{SO}_4^{\bullet-}$), is new type of oxidant used in in-situ chemical oxidation [18]. PS, including peroxymonosulfate (PMS) and peroxydisulfate (PDS), can be activated by ultraviolet light (UV) [19], ultrasound, heat [20], transition metal ions or their oxides [21–28], and nanocarbon [29–31]. Compared with hydroxyl radicals ($\bullet\text{OH}$), $\text{SO}_4^{\bullet-}$ has higher redox potentials ($E_0 = 2.60 \text{ V}$) at neutral pH value that can effectively remove organic contaminants in water via an oxidation reaction. UV-based AOPs have great potential due to their high treatment efficiency, non-toxicity and low cost. Many researchers [32,33] used the UV-activated persulfate process to study the removal of refractory organic pollutants. Since UV technology has been widely used in MWTPs, it is advantageous to use UV to activate persulfate. In this case, UV cannot only disinfect and sterilize the water [34], but also activate persulfate to produce strong oxidizing $\text{SO}_4^{\bullet-}$ to remove organic pollutants, thus it is more practical to study UV-activated persulfate to remove PABA-type UV filters [35]. However, previous studies have been mainly focused on the photocatalytic degradation of PABA [36–39] or ethyl 4-aminobenzoate (Et-PABA) [40], one of the typical PABA-type UV filters. Information regarding the $\text{SO}_4^{\bullet-}$ degradation process of Et-PABA is limited, which hinders the application of this technique in PABA-type UV filter treatments.

In this paper, the UV-activated PDS process was used to remove Et-PABA. The effects of PDS dosage, pH value, humic acid (HA) and other factors on the removal of Et-PABA during the UV/PDS process were investigated. The degradation intermediates of Et-PABA were identified and the possible degradation pathways were proposed. This work provides basic data, application references and theoretical guidance of the UV/PDS process for the removal of PABA-type UV filters in water.

2. Materials and Methods

2.1. Materials and Reagents

Et-PABA (99%) was provided by Macklin Biochemical Co., (Shanghai, China). Formic acid, methanol (MeOH), ethanol (EtOH), and *tert*-butanol (TBA) were HPLC grade and acquired from Sigma-Aldrich. Other reagents, such as peroxydisulfate (PDS), sodium chloride (NaCl), sodium nitrate (NaNO₃), sodium sulfate (Na₂SO₄), sodium hydrogen carbonate (NaHCO₃), potassium dihydrogen phosphate (KH₂PO₄), sodium hydroxide (NaOH), and sulfuric acid (H₂SO₄) were all analytical reagent (AR) grade, and were acquired from Aladdin (Shanghai, China).

2.2. Experimental Methods

A schematic diagram of the laboratory-made ultraviolet light irradiation device is shown in Figure 1. The size of the reactor was 30 × 30 × 30 cm. The ultraviolet light irradiator was equipped with two low-pressure mercury lamps (254 nm, G4T5, Philips, Kossaka, Poland; 4W). The UV lamps were arranged in parallel above a crystallizing dish (90 cm in diameter) and were approximately 10 cm from the surface of the solution, where the intensity of UV irradiation was determined by a digital UV-C meter (0.92 mW·cm⁻²). In order to ensure the stability of the light source, the UV lamps were preheated for 30 min. Generally, UV filters have been detected in water with concentrations up to µg/L. In this experiment, 0.05 mM of Et-PABA was chosen for convenience detection by LC and LC-MS [29,30]. 100 mL solution of Et-PABA and 2 mM PDS were added into a crystallizing dish, then magnetically stirred at 800 rpm. A quantity of 800 µL of the solution was sampled at different reaction times, filtered through a 0.45 µm filter, and added into 1.5 mL chromatography vials. The reaction was stopped with 200 µL of MeOH quencher.

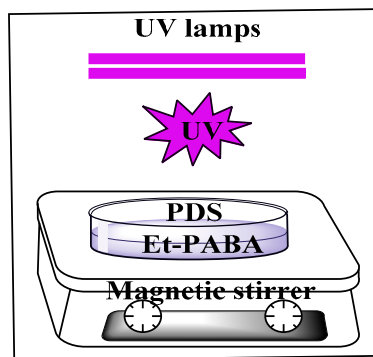


Figure 1. The apparatus used for the ethyl 4-aminobenzoate (Et-PABA) degradation.

2.3. Analysis Methods

The concentration of Et-PABA was determined by high-performance liquid chromatography (HPLC) equipped with an Zorbax SB-C18 column (4.6×250 mm, $5 \mu\text{m}$) (Agilent, Santa Clara, CA, USA). The chromatographic conditions were: Injection volume $10 \mu\text{L}$; flow rate 1.0 mL/min ; column temperature 30°C ; wavelength 282 nm ; mobile phase was methanol and formic acid solution (0.30%) mixed by a volume ratio of 4:6.

The removal efficiencies can be obtained by Equation (1).

$$r = \frac{C_0 - C}{C_0} \quad (1)$$

where, r is the removal efficiency; C_0 is the concentration of the original solution; C is the concentration of the solution after treatment using the oxidation process; and t is the reaction time.

The samples were extracted and enriched using Waters Oasis HLB columns (Waters, USA), and then were analyzed by an Qtrap 5600+ (AB Sciex, Redwood, CA, USA) MS coupled with an ESI source and an ACQUITY UPLC (Waters, Milford, MA, USA) [31].

3. Results and Discussion

3.1. Degradation of the Et-PABA Using Different Oxidation Processes

The removal efficiencies of Et-PABA using UV alone, the PDS alone and the UV/PDS combined process, respectively, were evaluated. As shown in Figure 2A, the removal efficiency of Et-PABA using a single UV process was only 23.7%, because the main ultraviolet radiation wavelength of 254 nm lies just within the absorption band of Et-PABA [32]. The UV process may cause photolysis of a part of Et-PABA because a small amount of active radicals such as $\bullet\text{OH}$ may be generated in the water to indirectly oxidize the contaminants [41]; the degradation efficiency of Et-PABA using the PDS process alone was only 21.2%, because PDS can theoretically oxidize and degrade parts of the organic compounds. By contrast, under the same reaction conditions, the removal efficiency of Et-PABA using the UV/PDS combined process increased rapidly, and the degradation efficiency can reach 98.7% in 30 min. The synergy value was calculated according to Reference [42]. It was a positive value (0.918), which stands for a synergistic effect that may greatly improve the removal efficiency of Et-PABA. $\text{SO}_4^{\bullet-}$ generated from the PDS activated by the ultraviolet light has a higher oxidation-reduction potential of $E_0 = 2.60 \text{ V}$, and its strong oxidizing ability can transform organic matter into an excited state and thus, the organic contaminants can be removed from water efficiently via an oxidation reaction [43]. Moreover, Figure 2B shows that the UV/PDS process can also efficiently remove PABA, indicating the universality of a UV/PDS process for the removal of PABA-type UV filters in water. Particularly, the degradation efficiencies of Et-PABA and PABA using the UV process were slightly higher than that using the PDS process after a 20 min reaction. This may be due to the fact that if UV radiation is increased or the reaction time is extended, UV alone can also remove contaminants from the water,

while PDS does not. Therefore, as time goes on, the individual UV process exhibits a better removal efficiency than the PDS alone. These results were consistent with the results of the previous study [32].

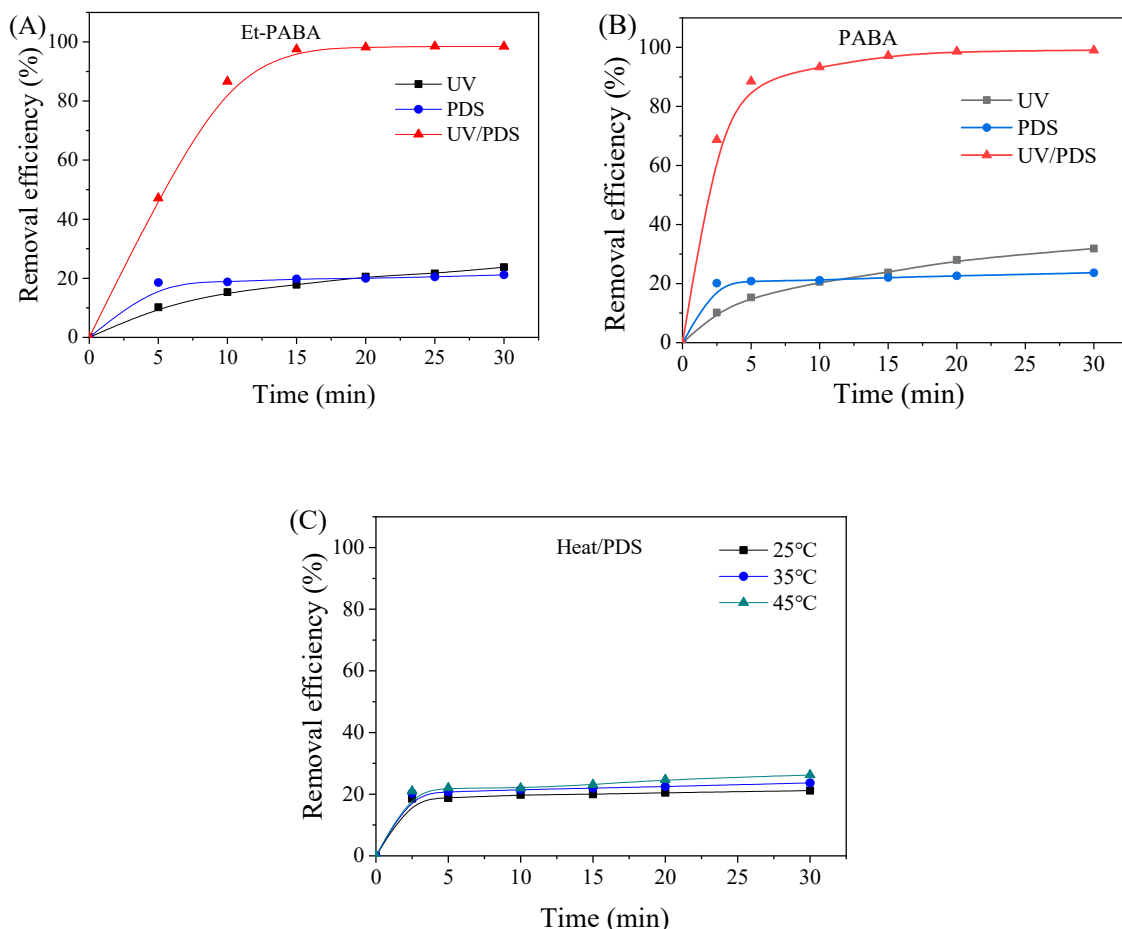


Figure 2. Removal efficiencies of (A) Et-PABA and (B) PABA using different oxidation processes; (C) removal efficiency of Et-PABA using persulfate (PDS) activated by heat energy. Conditions: $[Et\text{-PABA}] = [PABA] = 0.05 \text{ mM}$, $[PDS] = 2 \text{ mM}$, and without pH adjustment.

Subsequently, we also studied the removal efficiency of Et-PABA using PDS activated by heat energy. As shown in Figure 2C, the degradation rate did not increase significantly with the increase in the reaction temperature, mainly due to the relatively stable properties of PDS, thus PDS could not be activated by heat energy at low temperatures ($25\text{--}45^\circ\text{C}$) [44]. Dhaka et al. [32] also found the UV/PDS process was a time efficient process, compared to the heat-activated PDS oxidation of methyl paraben.

3.2. Effects of Various Factors on the Removal of Et-PABA

The concentration of oxidant dosage directly affects the amounts of free radicals produced; thus, it is necessary to study the effect of PDS dosage on the degradation of Et-PABA. As shown in Figure 3A, the degradation rate of Et-PABA increased as the concentrations of PDS increased from 1.0 to 4.0 mM within 15 min, which indicated that the removal of pollutants increased rapidly with the increase of oxidant dosage within a certain range. The main reason may be that as the concentration of PDS increases, the production of $\text{SO}_4^{\bullet-}$ and $\bullet\text{OH}$ free radicals also increases, which promotes the degradation efficiency of Et-PABA in a short time [45,46]. The remaining concentration of PDS (when adding 2.0 mM PDS) was determined using the iodometric titration method. The remaining rate was about 27%, indicating that increasing the oxidant dosage is effective but not economical.

Theoretically, 23.5 Mol of PDS is required to completely mineralize 1 Mol of Et-PABA. Thus, 2 mM of PDS (40:1) was chosen in this experiment, considering the actual excess consumption of oxidants.

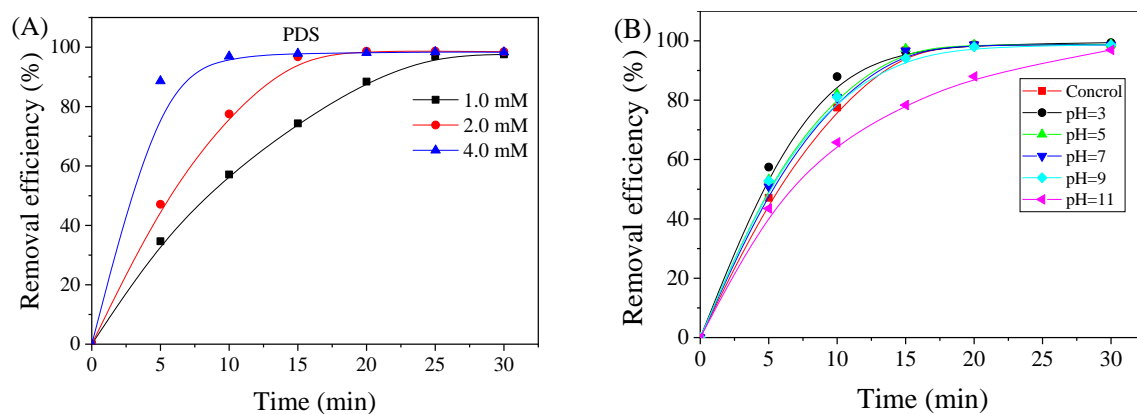


Figure 3. Effects of PDS dosage (A) and pH (B) on the removal efficiency of Et-PABA using UV/PDS. Conditions: [Et-PABA] = 0.05 mM, [PDS] = 2.0 mM, and without pH adjustment.

The acidity may affect the existence of free radicals in the UV/PDS process. Thus, the effect of pH on the Et-PABA removal was examined in this experiment. The initial pH values of the solution were adjusted from 3 to 11 with 0.1 M H_2SO_4 or 0.1 M NaOH, respectively, to investigate the impact of pH on the removal efficiency. As Figure 3B shows, the removal efficiency of Et-PABA was slightly better under acidic conditions, while it was slightly worse under the alkaline conditions in a short time of less than 20 min. It may be due to the existence of a large amount of H^+ in the reaction system which reacts with PDS to produce more $\text{SO}_4^{\bullet-}$, the predominate radicals in the UV/PDS system. $\text{SO}_4^{\bullet-}$ has a higher redox potential under acidic conditions, thereby accelerating the reaction rate [47]. Liang and coworkers found that acid-catalyzed decomposition of persulfate anion under acidic pH gives a higher concentration of $\text{SO}_4^{\bullet-}$ [48]. The slight decrease in the removal efficiency at pH 11 may be due to the fewer radicals generated as a result of the alkaline condition. However, as the reaction progressed, the final removal efficiency was greater than 97%, indicating that a wide range of pH value was applicable for the Et-PABA degradation using the UV/PDS process. From these results, the UV/PDS process is expected to be a prospective treatment in the remediation of emerging contaminants in wastewater.

In the case of scavenger reactions between the radicals generated during the UV/PDS process and the large number of anions in the natural water body such as Cl^- , NO_3^- , SO_4^{2-} , HCO_3^- , H_2PO_4^- , it is of great significance to investigate the effects of anions in water on the degradation of Et-PABA in the UV/PDS process [49]. To compare the effects of different anions on the degradation of Et-PABA, sodium chloride, sodium nitrate, sodium sulfate, sodium hydrogen carbonate, and sodium dihydrogen phosphate were added to the reaction system at a concentration of 5 mM [31], respectively. As shown in Figure 4A, Cl^- showed no inhibition effect on the decomposition, which may be due to the fact that Cl^- can react with sulfate radicals and produce relatively weak free radicals such as Cl^\bullet , Cl_2^\bullet and ClHO^\bullet [32]. HCO_3^- anions were thought to be scavengers of hydroxyl radicals that can react with sulfate radicals to produce bicarbonate radicals in the solution. Previous studies have shown that Cl^- and HCO_3^- at small concentrations can promote the degradation of organic compounds by the UV/PDS process [50]. The other ions, such as NO_3^- and SO_4^{2-} , had no significant effect on the removal efficiency of Et-PABA. Although most of the common ions in the water matrix may affect the degradation rate of Et-PABA, the removal efficiency of Et-PABA using the UV/PDS process in the presence of anions was still impressive when the reaction time increased to more than 20 min.

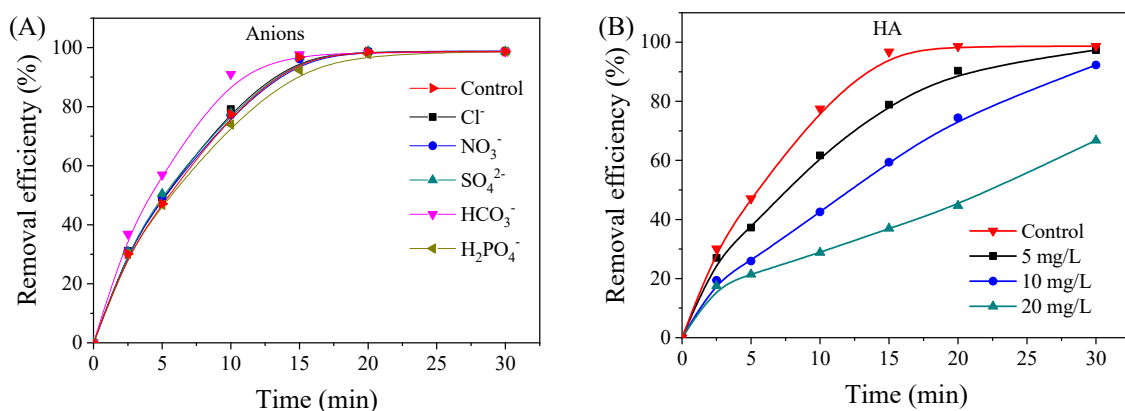


Figure 4. Effects of different anions (A) and humic acid (HA) concentrations (B) on the removal efficiency of Et-PABA. Conditions: [Et-PABA] = 0.05 mM, [anion] = 5 mM, [HA] = 5–20 mg/L, [PDS] = 2.0 mM, and without pH adjustment.

Humic acid (HA) is one of the main natural organic matter (NOM) in natural water. Thus, it's typically used as a representative of NOM to investigate the NOM effect on the UV/PDS oxidation process. Thus, the effects of HA at different concentrations on the removal of Et-PABA were investigated as shown in Figure 4B. The degradation rate of Et-PABA decreased with the increase in the HA concentration. The removal efficiencies at 30 min were 97.4%, 92.3%, and 66.8%, respectively, suggesting that HA had a significant inhibitory effect on the removal of Et-PABA. HA molecules contain a large amount of photosensitive substances such as aromatic carboxyl groups, hydroxyl groups, amine groups, which can directly absorb ultraviolet light, competitively inhibit the absorption of light energy by the PDS [51], and reduce the yield of free radicals in the solution. At the same time, the active group of HA will also compete with Et-PABA for active radicals such as SO₄^{•-}, thus reducing the removal efficiency of Et-PABA [52,53].

In order to study the degradation of Et-PABA in real water bodies, two water samples from different sources (river water and tap water from Jiaxing College) were collected and filtered through a 0.45 μm filter. In order to compare with the Et-PABA degradation in pure water, the same concentration of Et-PABA (0.05 mM) was added to the two real water samples, respectively. The effect of real water on the degradation of Et-PABA using the UV/PS process is shown in Figure 5. The degradation rate of Et-PABA in the tap water reached as high as 96.5% within 10 min, which was essentially the same as that in pure water. The degradation rate of Et-PABA in surface water decreased, but the removal efficiency also reached 94.3% after a reaction time of 20 min. This result may be attributed to the inhibition of NOM in the real water body and the interaction of other water components, as discussed above. These results suggest that the UV/PDS process has good adaptability regarding the Et-PABA removal of real water samples. Chen et al. [54] also studied the degradation of 2,4-dichlorophenol in the real water using the UV/PDS process. They determined the water quality of several real water bodies. The concentrations of Cl⁻, HCO₃⁻, and NO₃⁻ in different water samples were 42.5–63.0 mg/L, 128.0–136.6 mg/L, and 0.005–0.070 mg/L, respectively. The results also suggested the UV/PDS process can be further extended to practical applications.

3.3. Degradation Pathways

Figure 6 presents the possible transformation pathways of Et-PABA based on the six observed TPs. On one hand, SO₄^{•-} and •OH can directly attack the carbon on the benzene ring, resulting in hydroxylation of Et-PABA. Through this degradation pathway, TP1 was produced. This product was further hydroxylated to produce a product of TP2. On the other hand, TP3 was a product of Et-PABA formed after attacks by ROS caused the C–O bond between the carbonyl group and the ethoxy group to be broken. Under further actions of ROS, due to the oxidation or removal of the amino group, TP3

was converted into TP4 and TP6, respectively. Similarly, hydroxylation of TP4 produced TP5. Finally, these intermediates of Et-PABA can be further degraded to lower organic acids.

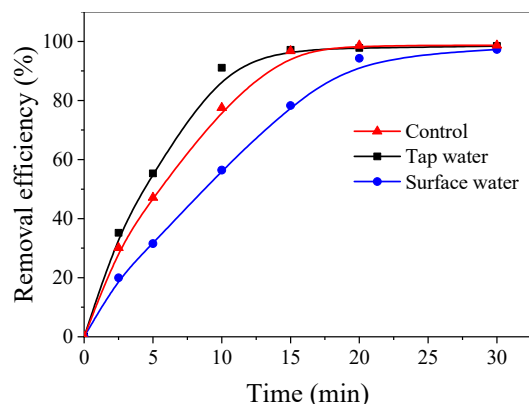


Figure 5. The degradation of Et-PABA in real water using the UV/PDS process. Conditions: [Et-PABA] = 0.05 mM, [PDS] = 2.0 mM, and without pH adjustment.

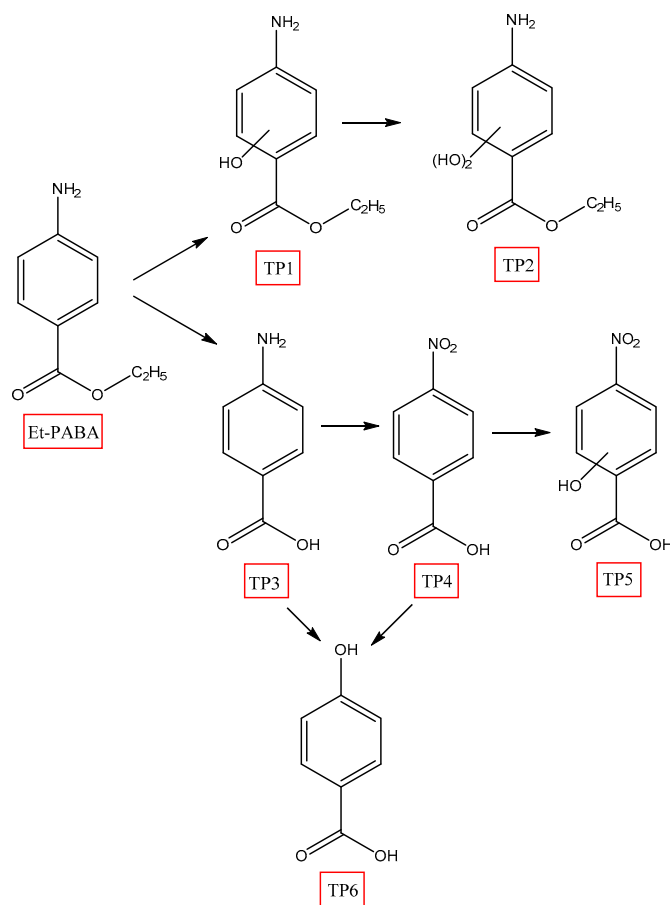


Figure 6. Proposed reaction pathways for the oxidation of Et-PABA using the UV/PDS process.

4. Conclusions

This study explored the removal efficiency, mechanism, and a novel advanced oxidation route for Et-PABA in a water environment using the UV/PDS combined process. The results showed that the combined treatment could significantly improve the degradation of Et-PABA compared to the single processes. The removal efficiency of Et-PABA after the UV/PDS combined process can reach 98.7% in 30 min. The removal rate of Et-PABA increased rapidly upon increasing the dosage of oxidant.

The presence of anions had no obvious effect on the removal, while HA suppressed the removal of Et-PABA. Moreover, the UV/PDS process had good adaptability to Et-PABA removal of real water samples. Finally, a degradation path of Et-PABA was proposed based on the six detected TPs during the oxidation process. Overall, the UV/PDS process can be used as a promising method for the removal of PABA-type UV filters in water.

Author Contributions: Conceptualization—Z.Z. and P.S.; Formal analysis—R.H. and Y.F.; Investigation—Q.W., C.L., and L.Z.; Supervision—H.L.; Validation—R.H. and J.W.; Writing of original draft—P.S.; Writing of review & editing—H.L.

Funding: This research was funded by the National Natural Science Foundation of China (21607058); the Zhejiang Provincial Department of Education General Research Project (Y201840526); the Student Research Innovation Team Funding Project of Zhejiang (2019R417027); the Student Research Training Program of Jiaxing University (2019); and the Key Project of Nanhu college of Jiaxing University (2018).

Acknowledgments: We wish to thank anonymous reviewers for their comments, which improved the paper greatly.

Conflicts of Interest: The authors declare no conflict of interest.

References

1. De Vries, E.; Arnold, M.; Altsitsiadis, E.; Trakatelli, M.; Hinrichs, B.; Stockfleth, E.; Coebergh, J. Potential impact of interventions resulting in reduced exposure to ultraviolet (UV) radiation (UVA and UVB) on skin cancer incidence in four European countries, 2010–2050. *Brit. J. Dermatol.* **2012**, *167*, 53–62. [[CrossRef](#)] [[PubMed](#)]
2. Liao, C.Y.; Kannan, K. Widespread occurrence of benzophenone-type UV light filters in personal care products from China and the United States: An assessment of human exposure. *Environ. Sci. Technol.* **2014**, *48*, 4103–4109. [[CrossRef](#)] [[PubMed](#)]
3. Krause, M.; Klit, A.; Jensen, M.B.; Soeborg, T.; Frederiksen, H.; Schlumpf, M.; Lichtensteiger, W.; Skakkebaek, N.E.; Drzewiecki, K.T. Sunscreens: Are they beneficial for health? An overview of endocrine disrupting properties of UV-filters. *Int. J. Androl.* **2012**, *35*, 424–436. [[CrossRef](#)] [[PubMed](#)]
4. He, K.; Hain, E.; Timm, A.; Tarnowski, M.; Blaney, L. Occurrence of antibiotics, estrogenic hormones, and UV-filters in water, sediment, and oyster tissue from the Chesapeake Bay. *Sci. Total Environ.* **2019**, *650*, 3101–3109. [[CrossRef](#)] [[PubMed](#)]
5. Mitchelmore, C.L.; He, K.; Gonsior, M.; Hain, E.; Heyes, A.; Clark, C.; Younger, R.; Schmitt-Kopplin, P.; Feerick, A.; Conway, A.; et al. Occurrence and distribution of UV-filters and other anthropogenic contaminants in coastal surface water, sediment, and coral tissue from Hawaii. *Sci. Total Environ.* **2019**, *670*, 398–410. [[CrossRef](#)] [[PubMed](#)]
6. Molins, D.D.; Munoz, R.; Nogueira, S.; Alonso, M.B.; Torres, J.P.; Malm, O.; Zioli, R.L.; Hauser-Davis, R.A.; Eljarrat, E.; Barcelo, D.; et al. Occurrence of organic UV filters and metabolites in lebranché mullet (*Mugil liza*) from Brazil. *Sci. Total Environ.* **2018**, *618*, 451–459. [[CrossRef](#)] [[PubMed](#)]
7. Apel, C.; Joerss, H.; Ebinghaus, R. Environmental occurrence and hazard of organic UV stabilizers and UV filters in the sediment of European North and Baltic Seas. *Chemosphere* **2018**, *212*, 254–261. [[CrossRef](#)]
8. Ao, J.; Yuan, T.; Gu, J.; Ma, Y.; Shen, Z.; Tian, Y.; Shi, R.; Zhou, W.; Zhang, J. Organic UV filters in indoor dust and human urine: A study of characteristics, sources, associations and human exposure. *Sci. Total Environ.* **2018**, *640*, 1157–1164. [[CrossRef](#)]
9. Liu, H.; Sun, P.; Liu, H.; Yang, S.; Wang, L.; Wang, Z. Acute toxicity of benzophenone-type UV filters for *Photobacterium phosphoreum* and *Daphnia magna*: QSAR analysis, interspecies relationship and integrated assessment. *Chemosphere* **2015**, *135*, 182–188. [[CrossRef](#)]
10. Liu, H.; Sun, P.; Liu, H.; Yang, S.; Wang, L.; Wang, Z. Hepatic oxidative stress biomarker responses in freshwater fish *Carassius auratus* exposed to four commonly benzophenone UV filters. *Ecotoxicol. Environ. Saf.* **2015**, *119*, 116–122. [[CrossRef](#)]
11. Li, A.; Law, J.; Chow, C.; Huang, Y.; Li, K.; Leung, K. Joint effects of multiple UV filters on zebrafish embryo development. *Environ. Sci. Technol.* **2018**, *52*, 9460–9467. [[CrossRef](#)] [[PubMed](#)]
12. Sun, X.; Wei, D.; Liu, W.; Geng, J.; Liu, J.; Du, Y. Formation of novel disinfection by-products chlorinated benzoquinone, phenyl benzoquinones and polycyclic aromatic hydrocarbons during chlorination treatment

- on UV filter 2,4-dihydroxybenzophenone in swimming pool water. *J. Hazard. Mater.* **2019**, *367*, 725–733. [CrossRef] [PubMed]
- 13. O’Malley, E.; O’Brien, J.W.; Tscharke, B.; Thomas, K.V.; Mueller, J.F. Per capita loads of organic UV filters in Australian wastewater influent. *Sci. Total Environ.* **2019**, *662*, 134–140. [CrossRef] [PubMed]
 - 14. Liu, H.; Sun, P.; He, Q.; Feng, M.; Liu, H.; Yang, S.; Wang, L.; Wang, Z. Ozonation of the UV filter benzophenone-4 in aquatic environments: Intermediates and pathways. *Chemosphere* **2016**, *149*, 76–83. [CrossRef] [PubMed]
 - 15. Binni, M.; Lu, G.; Liu, J.; Yan, Z.; Yang, H.; Pan, T. Bioconcentration and multi-biomarkers of organic UV filters (BM-DBM and OD-PABA) in crucian carp. *Ecotoxicol. Environ. Saf.* **2017**, *141*, 178–187.
 - 16. Suh, H.S.; Lim, S.K.; Kim, M.K.; Kim, M.H.; Baek, S.H. Risk assessment of ethylhexyl dimethyl PABA in sunscreen cosmetic products. *Toxicol. Lett.* **2017**, *280*, 105–106. [CrossRef]
 - 17. Guerra-Rodríguez, S.; Rodríguez, E.; Singh, D.N.; Rodríguez-Chueca, J. Assessment of sulfate radical-based advanced oxidation processes for water and wastewater treatment: A Review. *Water* **2018**, *10*, 1828. [CrossRef]
 - 18. Liu, H.; Bruton, T.A.; Doyle, F.M.; Sedlak, D.L. In situ chemical oxidation of contaminated groundwater by persulfate: Decomposition by Fe (III)-and Mn (IV)-containing oxides and aquifer materials. *Environ. Sci. Technol.* **2014**, *48*, 10330–10336. [CrossRef]
 - 19. Ye, J.; Zhou, P.; Chen, Y.; Ou, H.; Liu, J.; Li, C.; Li, Q. Degradation of 1H-benzotriazole using ultraviolet activating persulfate: Mechanisms, products and toxicological analysis. *Chem. Eng. J.* **2018**, *334*, 1493–1501. [CrossRef]
 - 20. Ji, Y.; Shi, Y.; Dong, W.; Wen, X.; Jiang, M.; Lu, J. Thermo-activated persulfate oxidation system for tetracycline antibiotics degradation in aqueous solution. *Chem. Eng. J.* **2016**, *298*, 225–233. [CrossRef]
 - 21. Xu, H.; Wang, D.; Ma, J.; Zhang, T.; Lu, X.; Chen, Z. A superior active and stable spinel sulfide for catalytic peroxyomonosulfate oxidation of bisphenol S. *Appl. Catal. B Environ.* **2018**, *238*, 557–567. [CrossRef]
 - 22. Alexopoulou, C.; Petala, A.; Frontistis, Z.; Drivas, C.; Kennou, S.; Kondarides, D.I.; Mantzavinos, D. Copper phosphide and persulfate salt: A novel catalytic system for the degradation of aqueous phase micro-contaminants. *Appl. Catal. B Environ.* **2019**, *244*, 178–187. [CrossRef]
 - 23. Deng, J.; Ya, C.; Ge, Y.; Cheng, Y.; Chen, Y.; Xu, M.; Wang, H. Activation of peroxyomonosulfate by metal (Fe, Mn, Cu and Ni) doping ordered mesoporous Co₃O₄ for the degradation of enrofloxacin. *RSC Adv.* **2018**, *8*, 2338–2349. [CrossRef]
 - 24. Li, R.; Cai, M.; Xie, Z.; Zhang, Q.; Zeng, Y.; Liu, H.; Liu, G.; Lv, W. Construction of heterostructured CuFe₂O₄/g-C₃N₄ nanocomposite as an efficient visible light photocatalyst with peroxydisulfate for the organic oxidation. *Appl. Catal. B Environ.* **2019**, *244*, 974–982. [CrossRef]
 - 25. Duan, X.; Su, C.; Miao, J.; Zhong, Y.; Shao, Z.; Wang, S.; Sun, H. Insights into perovskite-catalyzed peroxyomonosulfate activation: Maneuverable cobalt sites for promoted evolution of sulfate radicals. *Appl. Catal. B Environ.* **2018**, *220*, 626–634. [CrossRef]
 - 26. Ahn, Y.Y.; Bae, H.; Kim, H.I.; Kim, S.H.; Kim, J.H.; Lee, S.G.; Lee, J. Surface-loaded metal nanoparticles for peroxyomonosulfate activation: Efficiency and mechanism reconnaissance. *Appl. Catal. B Environ.* **2019**, *241*, 561–569. [CrossRef]
 - 27. Zhou, Y.; Wang, X.; Zhu, C.; Dionysiou, D.D.; Zhao, G.; Fang, G.; Zhou, D. New insight into the mechanism of peroxyomonosulfate activation by sulfur-containing minerals: Role of sulfur conversion in sulfate radical generation. *Water Res.* **2018**, *142*, 208–216. [CrossRef] [PubMed]
 - 28. Lin, C.; Shi, D.; Wu, Z.; Zhang, L.; Zhai, Z.; Fang, Y.; Sun, P.; Han, R.; Wu, J.; Liu, H. CoMn₂O₄ catalyst prepared using the sol-gel method for the activation of peroxyomonosulfate and degradation of UV filter 2-phenylbenzimidazole-5-sulfonic acid (PBSA). *Nanomaterials* **2019**, *9*, 774. [CrossRef] [PubMed]
 - 29. Liu, H.; Sun, P.; Feng, M.; Liu, H.; Yang, S.; Wang, L.; Wang, Z. Nitrogen and sulfur co-doped CNT-COOH as an efficient metal-free catalyst for the degradation of UV filter BP-4 based on sulfate radicals. *Appl. Catal. B Environ.* **2016**, *187*, 1–10. [CrossRef]
 - 30. Sun, P.; Liu, H.; Zhai, Z.; Zhang, X.; Fang, Y.; Tan, J.; Wu, J. Degradation of UV filter BP-1 with nitrogen-doped industrial graphene as a metal-free catalyst of peroxyomonosulfate activation. *Chem. Eng. J.* **2019**, *356*, 262–271. [CrossRef]

31. Sun, P.; Liu, H.; Feng, M.; Guo, L.; Zhai, Z.; Fang, Y.; Zhang, X.; Sharma, V.K. Nitrogen-sulfur co-doped industrial graphene as an efficient peroxyomonosulfate activator: Singlet oxygen-dominated catalytic degradation of organic contaminants. *Appl. Catal. B Environ.* **2019**, *251*, 335–345. [[CrossRef](#)]
32. Dhaka, S.; Kumar, R.; Khan, M.A.; Paeng, K.-J.; Kurade, M.B.; Kim, S.-J.; Jeon, B.-H. Aqueous phase degradation of methyl paraben using UV-activated persulfate method. *Chem. Eng. J.* **2017**, *321*, 11–19. [[CrossRef](#)]
33. Verma, S.; Nakamura, S.; Sillanpää, M. Application of UV-C LED activated PMS for the degradation of anatoxin-a. *Chem. Eng. J.* **2016**, *284*, 122–129. [[CrossRef](#)]
34. Moreno-Andrés, J.; Rios Quintero, R.; Acevedo-Merino, A.; Nebot, E. Disinfection performance using a UV/persulfate system: Effects derived from different aqueous matrices. *Photochem. Photobiol. Sci.* **2019**, *18*, 878–883. [[CrossRef](#)] [[PubMed](#)]
35. Xue, Y.; Dong, W.; Wang, X.; Bi, W.; Zhai, P.; Li, H.; Nie, M. Degradation of sunscreen agent p-aminobenzoic acid using a combination system of UV irradiation, persulphate and iron (II). *Environ. Sci. Pollut. Res.* **2016**, *23*, 4561–4568. [[CrossRef](#)] [[PubMed](#)]
36. Tsoumachidou, S.; Velegkaki, T.; Poulios, I. TiO₂ photocatalytic degradation of UV filter para-aminobenzoic acid under artificial and solar illumination. *J. Chem. Technol. Biotechnol.* **2016**, *91*, 1773–1781. [[CrossRef](#)]
37. Soto-Vazquez, L.; Cotto, M.; Duconge, J.; Morant, C.; Marquez, F. Synthesis and photocatalytic activity of TiO₂ nanowires in the degradation of p-aminobenzoic acid: A comparative study with a commercial catalyst. *J. Environ. Manag.* **2016**, *167*, 23–28. [[CrossRef](#)] [[PubMed](#)]
38. Zhou, L.; Ji, Y.; Zeng, C.; Zhang, Y.; Wang, Z.; Yang, X. Aquatic photodegradation of sunscreen agent p-aminobenzoic acid in the presence of dissolved organic matter. *Water Res.* **2013**, *47*, 153–162. [[CrossRef](#)]
39. Mao, L.; Meng, C.; Zeng, C.; Ji, Y.; Yang, X.; Gao, S. The effect of nitrate, bicarbonate and natural organic matter on the degradation of sunscreen agent p-aminobenzoic acid by simulated solar irradiation. *Sci. Total Environ.* **2011**, *409*, 5376–5381. [[CrossRef](#)]
40. Li, A.J.; Sang, Z.Y.; Chow, C.H.; Law, J.C.F.; Guo, Y.; Leung, K.S.Y. Environmental behavior of 12 UV filters and photocatalytic profile of ethyl-4-aminobenzoate. *J. Hazard. Mater.* **2017**, *337*, 115–125. [[CrossRef](#)]
41. Mc Kay, G.; Dong, M.; Kleinman, J.L.; Mezyk, S.P.; Rosario-Ortiz, F.L. Temperature dependence of the reaction between the hydroxyl radical and organic matter. *Environ. Sci. Technol.* **2011**, *45*, 6932–6937. [[CrossRef](#)] [[PubMed](#)]
42. Dewil, R.; Mantzavinos, D.; Poulios, I.; Rodrigo, M.A. New perspectives for advanced oxidation processes. *J. Environ. Manag.* **2017**, *195*, 93–99. [[CrossRef](#)] [[PubMed](#)]
43. Monteagudo, J.M.; Duran, A.; Gonzalez, R.; Exposito, A.J. In situ chemicaloxidation of carbamazepine solutions using persulfate simultaneously activated by heat energy, UV light, Fe²⁺ions, and H₂O₂. *Appl. Catal. B Environ.* **2015**, *176*, 120–129. [[CrossRef](#)]
44. Ji, Y.; Dong, C.; Kong, D.; Lu, J.; Zhou, Q. Heat-activated persulfate oxidation of atrazine: Implications for remediation of groundwater contaminated by herbicides. *Chem. Eng. J.* **2015**, *263*, 45–54. [[CrossRef](#)]
45. Zhang, R.; Sun, P.; Boyer, T.H.; Zhao, L.; Huang, C. Degradation of pharmaceuticals and metabolite in synthetic human urine by UV, UV/H₂O₂, and UV/PDS. *Environ. Sci. Technol.* **2015**, *49*, 3056–3066. [[CrossRef](#)]
46. Liu, Y.; He, X.; Fu, Y.; Dionysiou, D.D. Kinetics and mechanism investigation on the destruction of oxytetracycline by UV-254 nm activation of persulfate. *J. Hazard. Mater.* **2016**, *305*, 229–239. [[CrossRef](#)] [[PubMed](#)]
47. Romero, A.; Santos, A.; Vicente, F.; Gonzalez, C. Diuron abatement using activated persulphate: Effect of pH, Fe (II) and oxidant dosage. *Chem. Eng. J.* **2010**, *162*, 257–265. [[CrossRef](#)]
48. Liang, C.; Wang, Z.; Bruell, C.J. Influence of pH on persulfate oxidation of TCE at ambient temperatures. *Chemosphere* **2007**, *66*, 106–113. [[CrossRef](#)] [[PubMed](#)]
49. Martins, R.C.; Gmurek, M.; Rossi, A.F.; Corceiro, V.; Costa, R.; Quinta-Ferreira, M.E.; Ledakowicz, S.; Quinta-Ferreira, R.M. Application of Fenton oxidation to reduce the toxicity of mixed parabens. *Water Sci. Technol.* **2016**, *74*, 1867–1875. [[CrossRef](#)] [[PubMed](#)]
50. Tan, C.; Gao, N.; Deng, Y.; Zhang, Y.; Sui, M.; Deng, J.; Zhou, S. Degradation of antipyrine by UV, UV/H₂O₂ and UV/PS. *J. Hazard. Mater.* **2013**, *260*, 1008–1016. [[CrossRef](#)] [[PubMed](#)]
51. Khan, J.A.; He, X.; Khan, H.M.; Shah, N.S.; Dionysiou, D.D. Oxidative degradation of atrazine in aqueous solution by UV/H₂O₂/Fe²⁺, UV/S₂O₈²⁻/Fe²⁺ and UV/HSO₅/Fe²⁺ processes: A comparative study. *Chem. Eng. J.* **2013**, *218*, 376–383. [[CrossRef](#)]

52. Nie, M.; Yang, Y.; Zhang, Z.; Yan, C.; Wang, X.; Li, H.; Dong, W. Degradation of chloramphenicol by thermally activated persulfate in aqueous solution. *Chem. Eng. J.* **2014**, *246*, 373–382. [[CrossRef](#)]
53. Luo, C.; Ma, J.; Jiang, J.; Liu, Y.; Song, Y.; Yang, Y.; Guan, Y.; Wu, D. Simulation and comparative study on the oxidation kinetics of atrazine by UV/H₂O₂, UV/HSO₅[−] and UV/S₂O₈^{2−}. *Water Res.* **2015**, *80*, 99–108. [[CrossRef](#)] [[PubMed](#)]
54. Chen, J.; Gao, N.; Yang, J.; Wang, C.; Gu, Z.; Jiang, C. Study on the characteristics of 2,4-dichlorophenol in water degraded by UV/PS. *Chin. Environ. Sci.* **2017**, *37*, 2145–2149.



© 2019 by the authors. Licensee MDPI, Basel, Switzerland. This article is an open access article distributed under the terms and conditions of the Creative Commons Attribution (CC BY) license (<http://creativecommons.org/licenses/by/4.0/>).